APPLICATION OF HIGH SPEED AND HIGH EFFICIENCY HYDROGEN TURBOEXPANDERS IN REFINERY SERVICE

by

William A. Kardine

Sun Oil

Linwood, Pennsylvania

Reza Agahi

Executive Manager of Engineering

Behrooz Ershaghi

Development Manager

Atlas Copco Rotoflow

Gardena, California

and

Fouad Y. Zeidan

Director of Engineering

KMC, Inc.

Houston, Texas

William A. (Bill) Kardine is a Senior Mechanical Engineer with Sun Company Incorporated in Linwood, Pennsylvania. He has 25 years of experience in: the design and analysis of tooling for pump maintenance; ship spaces for engine and avionics support; oil, gas, and coal fired boilers; pump, compressor, and turbine systems; power plant equipment; flue gas power recovery equipment. He has additional experience as a consultant in the areas of: lubrication; vibration; equipment maintenance and repair; HVAC; spare parts analysis; and equipment reliability. His major areas of concentration have been in: power plant/cogen; major equipment; turbines, compressors, pumps; and spare parts management.

Mr. Kardine is a member of ASME and is a registered Professional Engineer in the Commonwealth of Pennsylvania.

Dr. Reza Agahi has received a B.S. and an M.S. (Mechanical Engineering) from Tehran University, an M.S. and a Ph.D. in Operations Research and Systems Engineering from the University of Southern California. Dr. Agahi has been with Atlas Copco Rotoflow since 1973, and he is presently the Executive Manager of Engineering of Atlas Copco Rotoflow. Dr. Agahi has taught in universities in Southern California and has authored over 30 papers and articles in operations research and turbomachinery applications. Dr. Agahi is the inventor and coinventor of several Atlas Copco Rotoflow patents.

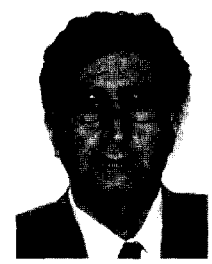

Dr. Behrooz Ershaghi received a B.S. and an M.S. (Chemical Engineering) from Tehran Polytechnic, an M.S. (Petroleum Engineering), and a Ph.D. (Chemical Engineering) from the University of Southern California. Dr. Ershaghi has been with Atlas Copco Rotoflow since 1974, and is presently the Development Manager of Atlas Copco Rotoflow. He has authored several papers and articles in turbomachinery applications. Dr. Ershaghi is coinventor of several Atlas Copco Rotoflow patents.

ABSTRACT

Turboexpander thermal efficiency is an important parameter in the process design of hydrogen purification plants. When a process requires low flow and high head, expander thermal efficiency can only be improved by increasing rotational speed. This trend towards higher speeds is often limited by the stability and rotordynamic characteristics of the rotor-bearing system. High rotational speeds necessitate the use of smaller diameter bearings to maintain acceptable surface speeds. Conventional tilt pad bearings cannot achieve the required clearance and preload due to the stackup of manufacturing tolerances inherent in their multi-piece design. A new style of tilting pad bearings which are manufactured using wire EDM technology, offered a solution to the size and stability problem.

Herein, the authors present an application of high-speed turboexpanders in a hydrogen purification process. The thermal efficiency of this system is approximately 20 percent better than the equipment it replaced. Some problems of a minor nature were experienced during the commissioning of these units and will be discussed along with the approach and solutions used to solve these problems.

INTRODUCTION

The application of turboexpanders to natural gas service in the early 1960s was a breakthrough in technology that smoothed the way to utilize this class of turbomachinery in the refrigeration of low molecular weight gases [1]. The first turboexpander application in a hydrogen gas process dates back to the late 1960s [2].

Stodola [3] has shown that turboexpander efficiency is a function of rotational speed. Balje [4] has proven that the optimal gas dynamic performance is at $U/C_0 = 0.7$ where U is tip speed of expander wheel and C_0 is spouting velocity equivalent to total head. Turboexpander manufacturers have learned that efficient expansion of hydrogen demands rotational speeds of 80 to 100,000 rpm. There were, however, two constraining factors; manufacturing of small diameter wheels, and small diameter high-speed bearing technology.

Casting of small diameter wheels was not feasible. Aluminum casting was even more troublesome than steel casting. Welded stainless steel wheels, although feasible, were not suitable due to their relatively heavy weight. Brazed aluminum wheels, on the other hand, could not be safely run at speeds that exceed 80,000 rpm. Modern 5-Axis NC milling technology has overcome these problems.

Sleeve bearing technology was limited in stability particularly at these relatively high speeds. Tilting pad bearing technology that theoretically offered more stability, was limited by the manufacturing tolerances that were not practical for the small size high-speed bearings. Their rotordynamic behavior under certain combinations of load and speed was not acceptable. To overcome such a drawback, it was necessary to acquire tilting pad type bearings that can be manufactured with a high precision in order to limit the manufacturing tolerances to acceptable values.

Turboexpander technology has become more mature in both gas dynamics and rotor bearing dynamics design aspects. Computational fluid dynamics (CFD) is utilized to design an optimal expander wheel. Advanced rotordynamics software is utilized to design an optimal rotor-bearing system free from critical speeds in the operating range of speed.

TURBOEXPANDER APPLICATION IN HYDROGEN LIQUEFACTION AND PURIFICATION

Due to the inversion temperature for hydrogen (204°K), hydrogen liquefaction is not feasible with a cascade process. Above this temperature, the Joule-Thompson effect reverses the sign and further expansion warms hydrogen rather than cooling it. This is why expansion of high-pressure hydrogen in refineries may ignite, unless it is mixed with methane to prevent inversion and provide the Joule-Thompson cooling effect [5].

Purification of hydrogen could be achieved by using a prechilled turboexpander cycle. The latter cycle normally consists of three or four stages of expansion due to high enthalpy drop. A simplified process flow diagram is shown in Figure 1.

In a prechilled turboexpander cycle, hydrogen is expanded and cooled in a closed loop until the expander discharge temperature is below 60°K. At this temperature, all the impurities are separated and purified hydrogen enters the hydrogen compressor. With this cycle, hydrogen purity of 99.99 percent has been obtained.

TURBOEXPANDER DESIGN FOR HYDROGEN PROCESS

In the prechilled turboexpander cycle, which is the subject of this report, four expanders were utilized. Design parameters are shown in Table 1 across the four expander stages.

The combination of low volume and high head indicates that optimum thermal efficiency can be obtained at a rotational speed above 95,000 rpm. Once this rotational speed is achieved, the turboexpander overall thermal efficiency will exceed 80 percent. This

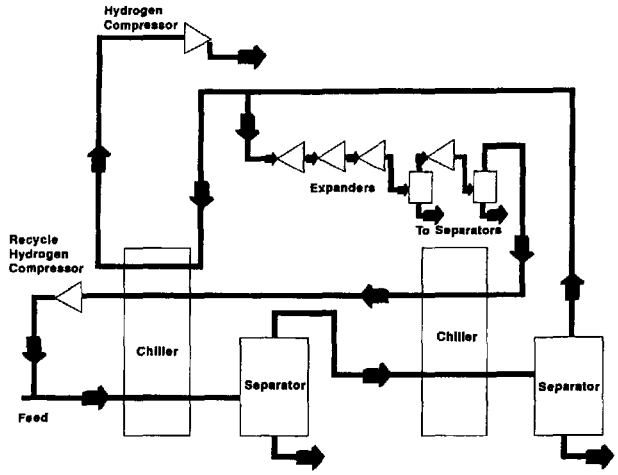

Figure 1. Simplified Process Flow Diagram.

Table 1. Design Parameters.

HEAD = 680 (Kj/Kg) EFFICIENCY = 80+ (%)

STAGE	#1	#2	#3	#4
P1 (psia)	400			
T1 (°F)	-275			
P2 (psia)				40
T2 (°F)				-360
Liquid (wt%)	0	0	1.5	4.0

efficiency also includes heat leakage from the cold box where the expander stages are installed.

The expander wheels are a radial inflow type designed for a condensing stream at the expander discharge with a specially patented blade design [6] that eliminates any performance penalty due to the condensing stream. The wheels are manufactured from an aluminum forging using CAD-CAM data transferred to high precision 5-Axis NC-milling machines.

The requirements for high head and low volume flow of hydrogen, condensation of hydrocarbons at the expander discharge, and the demand for high efficiency required a unique wheel design. The accurate prediction and identification of losses in a turboexpander highlight the areas where greater design efforts were concentrated. Focusing on these areas resulted in the highest reduction in losses and subsequently best efficiency.

Loss estimation is based on a component flow analyses. Main losses for this type of turbomachine are; primary expansion (guide vanes), secondary expansion (wheel), disk friction, seal losses, channel friction, diffusion or blade loading losses, leakage flow over guide vanes, heat leakage, incidence loss, and exit losses. The main losses and the percentage distribution are shown in Table 2.

Table 2. Hydrogen Turboexpander Losses.

Primary Expansion Guide Vanes (Nozzle)	**4.1%**
Secondary Expansion (wheel)	**1.2%**
Disk Losses	**3.0%**
Wheel Seal Losses	**1.2%**
Channel Friction Losses	**1.2%**
Inducer & Turning Losses	**1.0%**
Others	**0.3%**
Total Losses	**12.0%**

Most losses are a function of gas velocity distribution through the wheel. The basic equation for velocity distribution within the blades is as follows [7]:

$$\frac{dw}{dn} = EW - G \quad (1)$$

where $\frac{dw}{dn}$ is the rate of change of relative velocity along a normal to the meridional streamlines, E is the geometric function and G is the fluid dynamic function. Since the values of E and G vary along the hub or shroud, closed form integration is very involved and hence the equation is integrated numerically. The integration proceeds from streamline to streamline, beginning with either the hub or the shroud starting streamline.

Modern design technology allows the designer to modify the blade geometries for minimum losses while maintaining low stress levels and avoiding blade resonances. Surface velocities are shown in Figures 2 and 3 along the hub and shroud camberline distances of the last stage expander. In order to reduce the stress at high rotational speeds, the expander wheels are made with radially elemented blades.

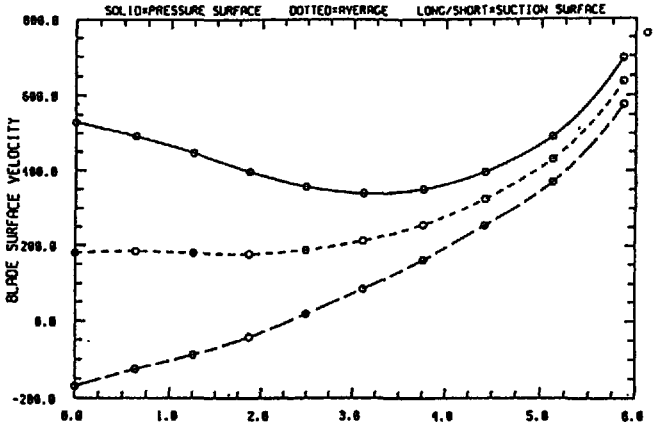

Figure 2. Camberline Distance Loading Diagram at Hub Streamtube.

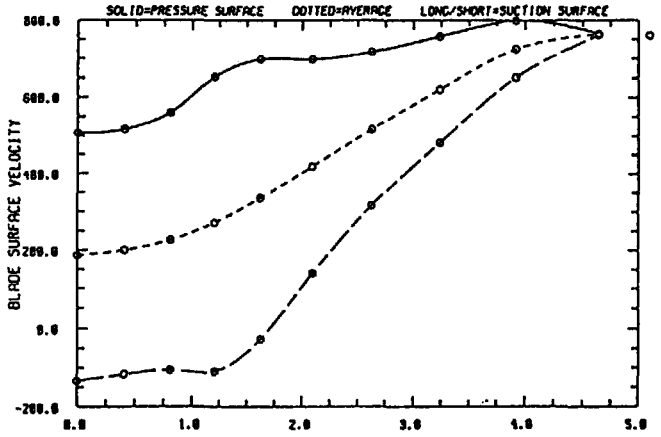

Figure 3. Camberline Distance Loading Diagram at Shroud Streamtube.

The turboexpander shown in Figure 4 is equipped with variable geometry inlet guide vanes (IGV) to keep performance reasonably flat in the range of operating process conditions, as shown in

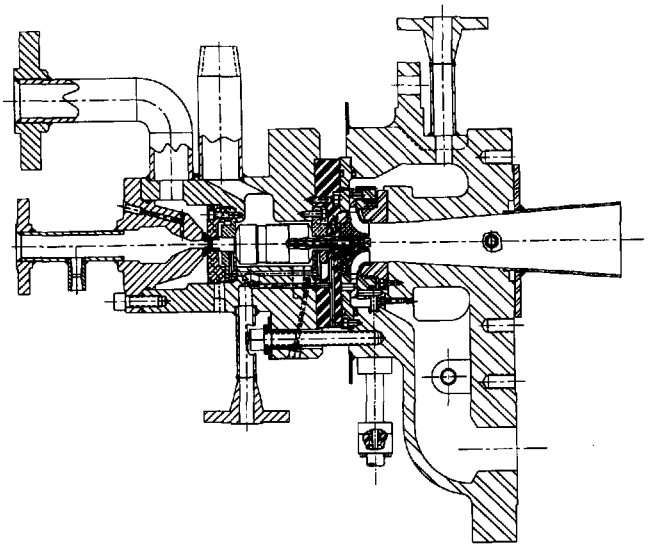

Figure 4. Turboexpander Cross Section.

Figure 5. The IGV segments are designed based on velocity triangle match to the wheel thus avoiding shock wave turbulence at the wheel entry.

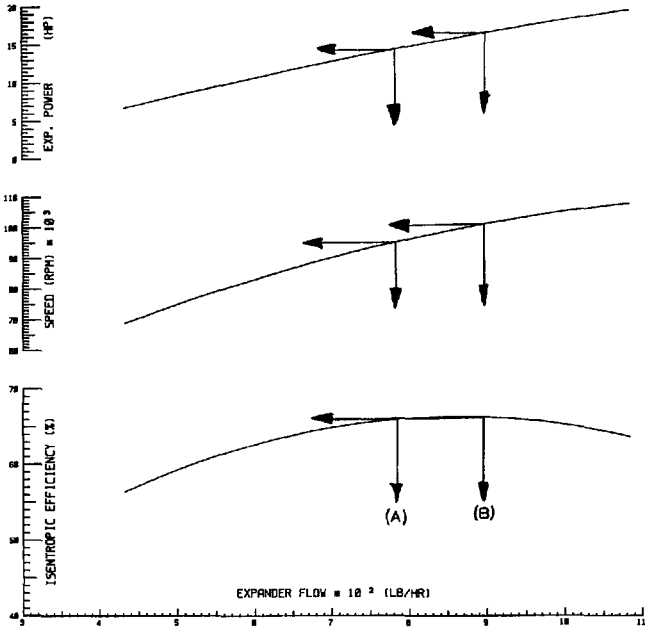

Figure 5. Performance Curves of the First Stage Turboexpander.

Due to low mechanical power produced by the turboexpander, mechanical energy is absorbed in a closed loop oil brake system. The oil brake loop can be adjusted for oil flow or head to provide variable load and hence an optimal loading for the expander. This variable load mechanism enables the process to adjust the turboexpander speed and in turn maximizes thermal efficiency of the expanders. The oil brake is designed to prevent cavitation at high rotational speeds.

Shaft material is chosen to be compatible with the cryogenic temperature of the expander process. Continuous flow of seal gas is provided to prevent cryogenic process gas from entering the bearing housing and/or oil mist migration to the cryogenic process.

BEARING SELECTION AND ROTORDYNAMICS

Bearing Review and Selection

The trend towards higher speed and efficiency in modern turbomachinery has resulted in increasingly more demanding performance from fluid film bearings. While conventional tilt pad bearings have been able to provide an inherently stable design, their lower direct damping is often insufficient to suppress other destabilizing forces present in the novel and more modern turbomachinery. Furthermore, conventional tilt pad bearings have other limitations that are more obscure than those noted with sleeve bearings. These problems may not become apparent until the bearings have been in service for some time.

Conventional tilt pad bearings are comprised of different parts that are assembled together. Each part has manufacturing tolerances associated with its critical dimensions. As a result, the critical speed and stability can vary over a wide range making it difficult to meet certain specific performance requirements. Another limitation is pad flutter and instability which has in the past prevented the use of four and three-pad bearings on high-speed turbomachinery in spite of their better rotordynamic characteristics.

The difficulty in attaining close tolerance bearing clearances and preloads with conventional style tilt pad bearings is one of the major factors for the inaccuracies often encountered in predicting stability and critical speeds. The manufacturing tolerances result in progressive widening of the clearance and preload spread as the bearing size reduces. The manufacturing tolerances associated with a conventional tilt pad bearing are shown in Figure 6. Although these tolerances are relatively small, their stackup in an assembly can result in a significant spread in the set bore clearance and preload. The minimum and maximum preloads shown in Table 3 are determined for the 0.625 in bearing used in this application. The spread in preload can have a serious effect on the stability of the rotor-bearing system. This is one of the reasons why the latest API specifications for centrifugal compressors (API 617 5th ed.) and steam turbines (API 612 3rd ed.) specifically address the need to evaluate the rotor-bearing performance at both the minimum, maximum, along with the nominal clearance and preload.

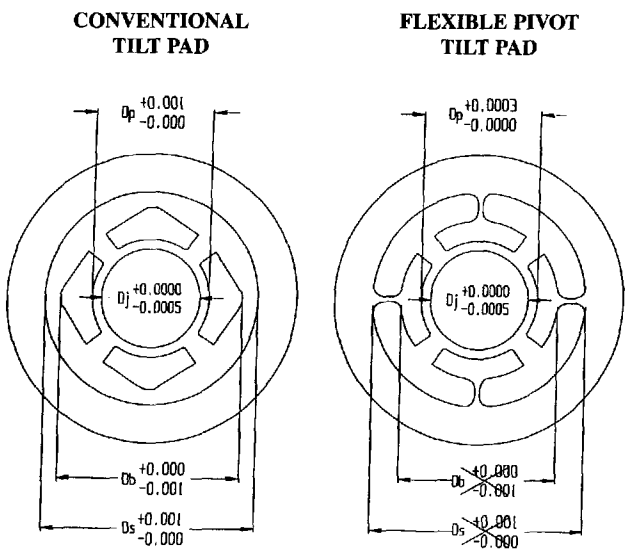

Figure 6. Comparison Between Conventional Tilt Pad and Flexible Pivot Bearing.

The manufacturing tolerances for a comparable flexible pivot tilt pad bearing are shown in the right column of Table 3. The geometric configuration of this bearing style and the manufacturing technique which uses state of the art wire electric discharge machining (EDM) eliminates the stackup in manufacturing tolerances. The precision accessible with the latest wire EDM CNC manufacturing technology expands the practical use of tilting pad bearings to smaller bearing sizes. Furthermore, the set bore and the pad bore in flexible pivot bearings are obtained during the same cutting process and not separately, as is the case with conventional tilt pad bearings. Therefore, the manufacturing tolerances are further reduced since the pad bore and set bore are not independently acquired. This was crucial in the case of this high-speed turboexpander application which is rated at a maximum continuous speed of 105,000 rpm and has a shaft diameter of only 0.625 in at the bearing location.

Table 3. Calculation of Minimum and Maximum Preload for a 0.625 in Bearing.

$$Preload = M = 1 - \frac{C_b}{C_p} = 1 - \frac{D_b - D_s}{D_p - D_s} = \frac{D_p - D_b}{D_p - D_s}$$

C_b = Bearing Set Clearance C_p = Pad Machined Clearance

D_{smax} = Maximum Shaft Diameter = 0.6250

D_{smin} = Minimum Shaft Diameter = 0.6247

CONVENTIONAL TILT PAD BEARING	FLEXIBLE PIVOT TILT PAD BEARING
D_{bmin} = Bearing Set Bore$_{min}$ = 0.62625	D_{bmin} = Bearing Set Bore$_{min}$ = 0.6267
D_{bmax} = Bearing Set Bore$_{max}$ = 0.62725	D_{bmax} = Bearing Set Bore$_{max}$ = 0.6270
D_{pmin} = Pad Machined Bore$_{min}$ = 0.6271	D_{pmin} = Pad Machined Bore$_{min}$ = 0.62760
D_{pmax} = Pad Machined Bore$_{max}$ = 0.6281	D_{pmax} = Pad Machined Bore$_{max}$ = 0.62790
$Preload_{min} = \frac{D_{p_{min}} - D_{b_{max}}}{D_{p_{min}} - D_{s_{max}}}$	$Preload_{min} = \frac{D_{p_{max}} - D_{b_{max}}}{D_{p_{max}} - D_{s_{min}}}$
$Preload_{max} = \frac{D_{p_{max}} - D_{b_{min}}}{D_{p_{max}} - D_{s_{max}}}$	$Preload_{max} = \frac{D_{p_{min}} - D_{b_{min}}}{D_{p_{min}} - D_{s_{max}}}$
$M_{min} = \frac{0.6271 - 0.62725}{0.6271 - 0.62625}$	$M_{min} = \frac{0.6279 - 0.6270}{0.6279 - 0.6247}$
$M_{min} = -0.057$	$M_{min} = 0.281$
$M_{max} = \frac{0.6281 - 0.62625}{0.6281 - 0.625}$	$M_{max} = \frac{0.6276 - 0.6267}{0.6276 - 0.6250}$
$M_{max} = 0.596$	$M_{max} = 0.346$

The introduction of rotational stiffness in the pivot structure which is inherent in the design of flexible pivot bearings, will raise the pad flutter threshold instability and allow the use of fewer pads in a given bearing configuration. These bearings possess all the favorable characteristics of conventional tilt pad bearings without any of their drawbacks.

Turboexpander Rotor Model

The rotor model for this high-speed turboexpander is shown in Figure 7. The bearings are indicated by the spring elements and are modelled as forces acting on the rotor at their respective location. The operating speed range for this expander was relatively wide, varying from 60,000 to 105,000 rpm. It was crucial to provide a reliable rotor-bearing system design with no critical speeds in the operating speed range. Furthermore, the stability of the first two rigid modes must be high enough to suppress the potential for any subsynchronous vibrations.

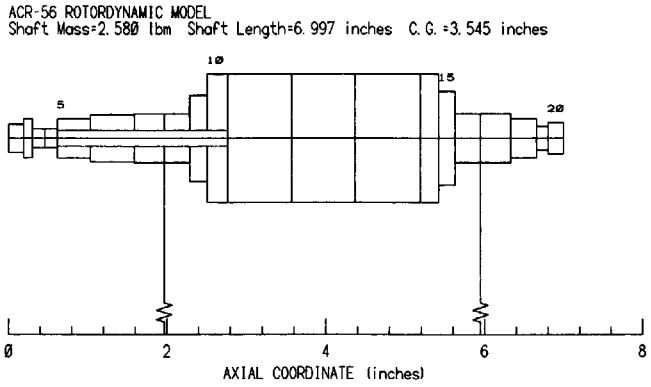

Figure 7. Rotor Model.

Undamped Critical Speed Map

The undamped critical speed map was generated for this rotor and is shown in Figure 8. Superimposed on the critical speed map are the bearing stiffness coefficients and the running speed range. The intersection of the bearing stiffness with the critical speed lines indicates the potential for exciting critical speeds. The speed dependent bearing stiffness shows that the rotor bearing system will pass through the first and second critical speeds as the rotor accelerates towards the operating speed range.

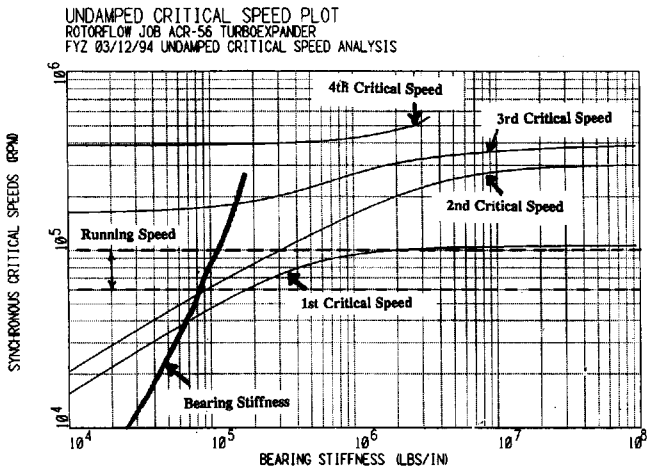

Figure 8. Undamped Critical Speed Plot.

The running speed appears to be adequately separated from the second and third critical speeds. Furthermore, the bearing coefficients intersect the critical speed lines (first and second) in the sloping section of the curves. This indicates that the bearings are soft relative to the shaft, resulting in adequate motion at the bearings which will provide more effective bearing damping for these two modes. Even though the second mode appears to be close to the minimum operating speed, the unbalance response and stability analysis discussed next verify that this mode is critically damped and no peak response was evident in the analysis or testing. This relatively stiff rotor in comparison with flexibility of the bearings was key to the success in achieving the rotordynamic characteristics sought in this application. The first true flexible mode (third natural frequency) is adequately separated from the maximum operating speed due to the stiff rotor design.

Stability Analysis

Stability is one of the main considerations in the design and operation of high-speed turbomachinery. Although the rotor bearing system for this expander does not have a flexible mode below or within the operating speed range, it does have two rigid modes which must be adequately damped to prevent the potential for subsynchronous vibrations.

The damped eigenvalue analysis was performed with an optimized set of flexible pivot bearings. The first forward mode is shown in Figure 9 along with the logarithmic decrement for that mode. The logarithmic decrement which is often abbreviated as log. dec. is a measure used to gauge the stability of the rotor-bearing system. A positive log. dec. means that any free vibrations of the system will damp out with time in the event of any excitation or perturbation of the system resonances. A negative log. dec. means that the vibrations will grow with time which is indicative of an unstable rotor-bearing system. The second mode is shown in Figure 10 and has a relatively high log. dec. value. A log. dec. above 1.0 will often result in a critically damped mode. The third mode shown in Figure 11, is a flexible mode. This mode will have significant shaft bending. However, its frequency is much higher than the operating speed and therefore will not be of any consequence for this turboexpander application.

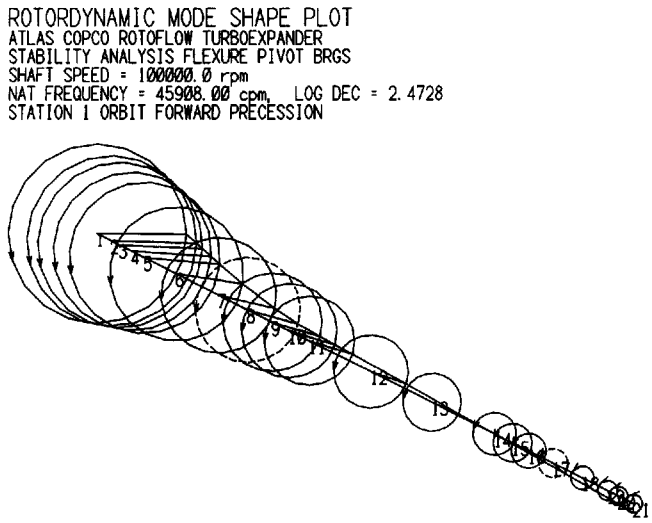

Figure 9. Rotordynamic Mode Shape Plot.

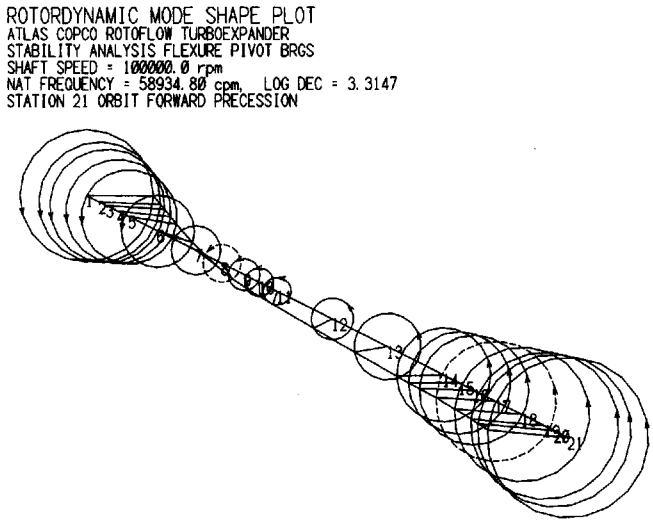

Figure 10. Rotordynamic Mode Shape Plot.

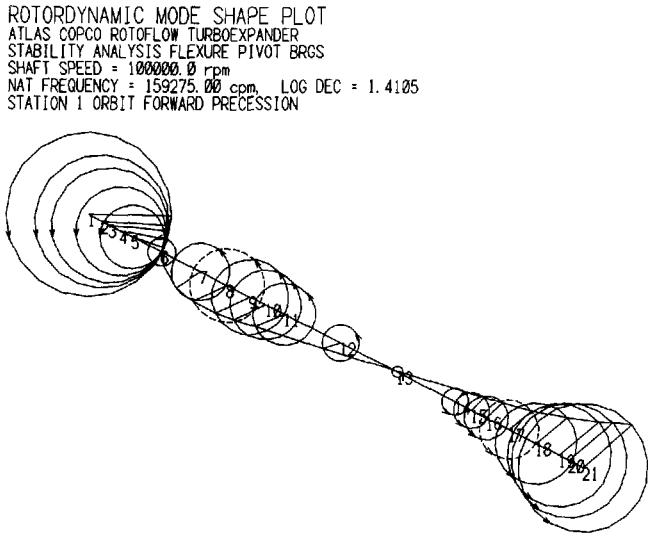

Figure 11. Rotordynamic Mode Shape Plot.

Unbalance Response Analysis

The response to unbalance was evaluated in order to verify the critically damped modes predicted in the eigenvalue analysis and to determine the location of the critical speeds. The response at the two bearings are shown in Figures 12 and 13, respectively. The response confirmed that the first two rigid modes are critically damped. As expected, no peak responses can be found within the operating speed range. Testing at the turboexpander manufacturer's site also collaborated these results and established the reliability and robustness of this rotor-bearing system. A photograph is shown in Figure 14 of the flexible pivot tilt pad bearing used in this application.

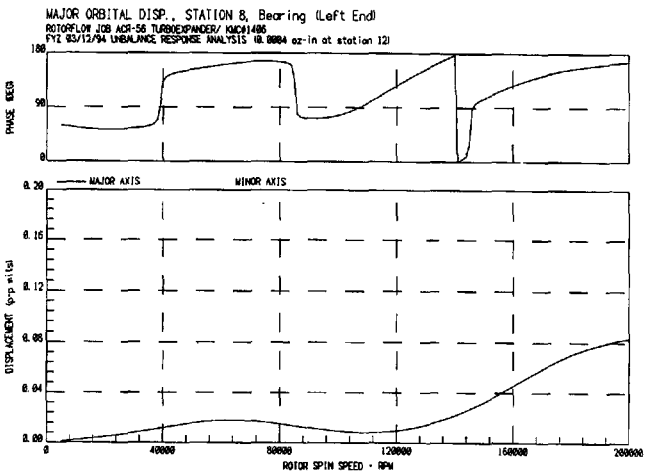

Figure 12. Major Orbital Displacement (Expander Bearing).

SHOP MECHANICAL TESTING

The high-speed turboexpanders were tested at the manufacturer's test facility to verify the mechanical integrity and some of the critical performance characteristics. The units were tested with air and key operating parameters such as speed, vibration, and lubricating oil temperature at the inlet and outlet of the bearings were recorded as shown in Table 4. The temperature rise across the

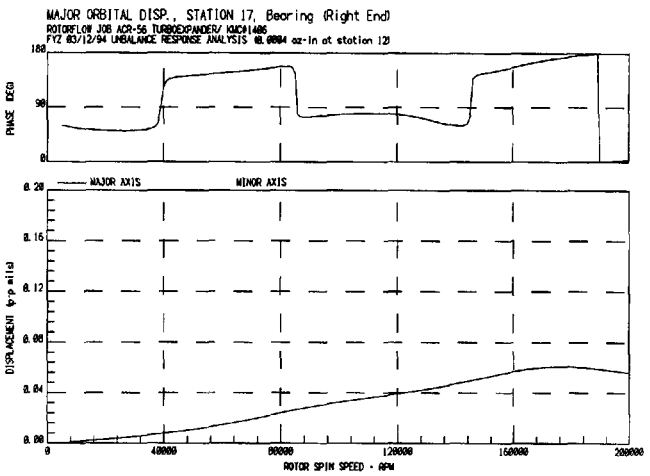

Figure 13. Major Orbital Displacement (Oil Brake Bearing).

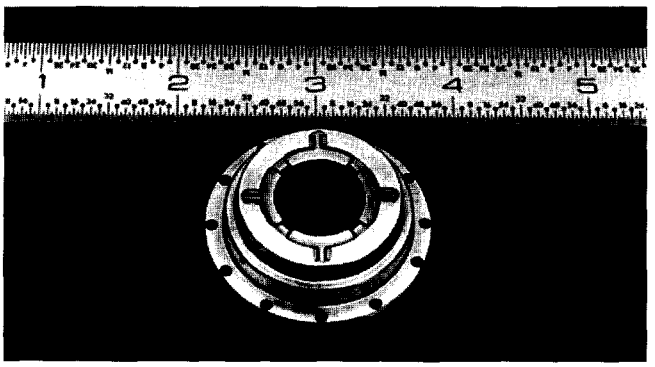

Figure 14. Flexure Pivot Bearing.

Table 4. Mechanical Running Test.

	UNIT # 2	UNIT # 3
SPEED (RPM)	105,000	106,000
BRG. OIL INLET (°F)	104	96
BRG. OIL OUTLET (°F)	132	128
VIB. DRIVE END BRG (Horizontal) (MILS)	0.1	0.1
VIB. DRIVE END BRG (Vertical) (MILS)	0.1	0.1
VIB. LOAD END BRG (Horizontal) (MILS)	0.1	0.25
VIB. LOAD END BRG (Vertical) (MILS)	0.1	0.25

bearings was within the design range of 30°F. The vibrations were very low as the shaft traversed the first two critically damped rigid modes. The steady state readings at 105,000 and 106,000 rpm were also very low as shown in the table indicating a well balanced rotor and adequate separation from any critical speed.

FIELD PERFORMANCE

This turboexpander package was commissioned in the Fall of 1994. The commissioning process was smooth and for the most part trouble free. However, a few unforeseen problems were expe-

rienced and will be discussed in this section. Solutions to the commissioning problems are also presented.

Impurity in Seal Gas

This turboexpander package was designed for relatively pure hydrogen to be used as seal gas. However, at startup, hydrogen with high purity was not available. Supply of seal gas with high (5-10 mole percent) methane content resulted in accumulation of frozen methane in the interstage piping and subsequent blockage of flow. This, in turn, resulted in a speed reduction for the second, third, and fourth stage expanders. As a result, efficiency of the turboexpander cycle was affected and hence hydrogen purification was not as effective as originally anticipated. This meant that pure seal gas could not be supplied and hence this situation was permanent rather than being transitional. This problem was overcome by supplying seal gas with high purity at startup from a source independent of the expander cycle.

Seal Gas Pressure Control

Since seal gas flows against expander back wheel pressure, it is conceivable to adjust seal gas pressure in reference to expander back wheel pressure. Supply of seal gas pressure control based on differential pressure ensures minimum seal gas flow and, hence, minimal thermal efficiency deterioration and thus reduction of operational cost.

During commissioning, due to high impurities in the seal gas, as was explained above, the expander back wheel pressure sensing line was also blocked with frozen methane. Therefore, seal gas supply pressure was not consistent with back wheel pressure and resulted in expander efficiency deterioration or cryogenic gas migration to the warm bearing housing. This problem was solved by taking a reference pressure tap from the expander discharge and re-setting the seal gas pressure accordingly.

CONCLUSIONS

This application demonstrated a successful application of high-speed and high-efficiency turboexpanders in process plants. Advanced analytical tools have enabled designers to design inlet guide vanes and wheels with minimum dynamic and frictional losses. CNC machine tools have made machining of a wheel from a solid piece possible. Advanced fluid film bearing technology is now available for turbomachines operating at 100,000 rpm without any instability.

In spite of the minor problems experienced in the commissioning of these units, this application demonstrated that the technology for high-speed turboexpanders had matured. Since this application, there have been several similar turboexpander applications with similar speeds and efficiencies.

REFERENCES

1. Swearingen, J. S., "Turboexpander and Process That Use Them," Chemical Engineering Progress, *68,* (7) (1972).
2. Agahi, R. R., et al., "High Performance Cryogenic Turboexpander," CEC/ICMC, Columbus, Ohio (1995).
3. Stodola, A., "Steam & Gas Turbines," Peter Smith (1995).
4. Balje, O. E., *Turbomachine,* New York, New York: John Wiley and Sons (1981).
5. ASHRE data book, *1,* (1), Section 45 (1959).
6. Swearingen, J. S., U.S. Patent Number 3610775 (1971).
7. NREC, "An Interactive Graphics System for the Design of Radial Turbomachinery," (1991).